Cell, Vol. 99, 781–790, December 23, 1999, Copyright ©1999 by Cell Press

The Ephrin VAB-2/EFN-1 Functions in Neuronal Signaling to Regulate Epidermal Morphogenesis in *C. elegans*

Ian D. Chin-Sang, Sean E. George, Mei Ding, Sarah L. Moseley, Andrew S. Lynch, and Andrew D. Chisholm*
Department of Biology
Sinsheimer Laboratories
University of California
Santa Cruz, California 95064

Summary

The Eph receptor VAB-1 is required in neurons for epidermal morphogenesis during *C. elegans* embryogenesis. Two models were proposed for the nonautonomous role of VAB-1: neuronal VAB-1 might signal directly to epidermis, or VAB-1 signaling between neurons might be required for epidermal development. We show that the ephrin VAB-2 (also known as EFN-1) is a ligand for VAB-1 and can function in neurons to regulate epidermal morphogenesis. In the absence of VAB-1 signaling, ephrin-expressing neurons are disorganized. *vab-2/efn-1* mutations synergize with *vab-1* kinase alleles, suggesting that VAB-2/EFN-1 may partly function in a kinase-independent VAB-1 pathway. Our data indicate that ephrin signaling between neurons is required nonautonomously for epidermal morphogenesis in *C. elegans*.

Introduction

Epithelial cells display many types of morphogenetic behavior. A common type of epithelial morphogenesis is the spreading of an epithelial sheet over a substrate, as in embryonic epiboly and wound closure (Bard, 1992). Epibolic movements may be driven by cell proliferation or changes in cell shape, and have been described in the embryos of many animal phyla. Dorsal closure of the *Drosophila* epidermis is a well-studied example of epiboly. Many genes have been identified that function in dorsal closure, including the myosin *zipper*, components of a MAP kinase/JNK signal transduction pathway that functions in the leading edge cells, and components of a TGFβ pathway required to transduce signals from the leading edge cells (reviewed in Noselli and Agnes, 1999). Epiboly in the zebrafish requires the Jak1 kinase (Conway et al., 1997); several genes required for zebrafish epiboly have also been isolated in genetic screens (Kane et al., 1996; Solnica-Krezel et al., 1996).

The epidermis of the nematode *C. elegans* is an epithelium that undergoes epiboly during embryogenesis, where it encloses the embryo ventrally (Sulston et al., 1983). Ventral enclosure is the result of epidermal cell shape changes (Williams-Masson et al., 1997) and involves two steps: first, the extension of four anterior leading cells to the ventral midline, and second, enclosure of the posterior epidermis. A catenin/cadherin system is required for normal movement of the anterior epidermal cells, and likely functions within epidermal cells to modulate cytoskeletal behavior (Costa et al., 1998).

We reported previously that the *vab-1* (*vab*, *v*ariable *ab*normal) gene functions in two phases of embryonic morphogenesis: first, in the movement of neuroblasts during closure of the ventral gastrulation cleft, and second, in epidermal ventral enclosure (George et al., 1998). *vab-1* encodes a *C. elegans* Eph receptor tyrosine kinase, and is required nonautonomously in the nervous system for normal epidermal development. Vertebrate Eph receptors bind ligands known as ephrins (reviewed in Flanagan and Vanderhaeghen, 1998). Ephrin/Eph receptor signaling functions in many diverse processes (reviewed by Holder and Klein, 1999), including axon guidance, somitogenesis, angiogenesis, neural crest cell migration (Krull et al., 1997; Smith et al., 1997), and cell sorting during segmentation of rhombomeres (Xu et al., 1999). Vertebrate ephrins are either membrane anchored by a glycosylphosphatidylinositol (GPI) anchor (ephrin-As) or are transmembrane proteins (ephrin-Bs). Ephrin-Bs become phosphorylated on cytoplasmic tyrosyls in response to receptor binding (Holland et al., 1996; Brückner et al., 1997). EphB receptors thus function as bidirectional signaling molecules, with both "forward" (kinase-dependent) signaling and "reverse" (kinase-independent) signaling via ephrin-B ligands (Henkemeyer et al., 1996). Mutations that affect the kinase domain of VAB-1 do not cause complete loss of function, suggesting that VAB-1 might also have both kinase-dependent and kinase-independent functions.

VAB-1 is mainly expressed in the nervous system and loss of *vab-1* function in neurons causes defects in epidermal morphogenesis (George et al., 1998). We proposed two models for this nonautonomous role of VAB-1. In a "steric hindrance" model, VAB-1 signaling operates between neurons; lack of VAB-1 leads to disorganization of neurons, and epidermal cells are unable to migrate normally over this substrate. In a "reverse signal" model, VAB-1 signals from neurons to ligand-expressing epidermal cells. To distinguish between these models, we sought ligands for VAB-1. Here we show that the *vab-2* gene is also required for neural and epidermal morphogenesis and encodes a *C. elegans* GPI-anchored ephrin, also known as EFN-1. VAB-2/EFN-1 is expressed in neurons adjacent to VAB-1-expressing neurons, and not in epidermal cells. Analysis of *vab-1; vab-2* double mutants suggests that, unexpectedly, VAB-2/EFN-1 may partly function in a kinase-independent VAB-1 pathway.

Results

vab-2 Encodes a *C. elegans* Ephrin

We anticipated that mutations in ligands for VAB-1 might cause similar phenotypes to those of *vab-1* mutants.

*To whom correspondence should be addressed (e-mail: chisholm@biology.ucsc.edu).

Table 1. Strength of *vab-2/efn-1* Mutations and Molecular Lesions

Allele	Embryonic Arrest	Larval Arrest	Adult, Vab	Adult, Non-Vab	Wild-Type Sequence	Mutant Sequence	Effect
Strong							
ut78	8.4%	25.7%	38.7%	27.1%	CAA	**T**AA	Q8ochre
e2640	10.2%	24.2%	34.0%	31.6%	CAA	**T**AA	Q27ochre
ju1	11.9%	19.2%	45.0%	24.0%	TGG	TG**A**	W30opal
n1443	12.3%	18.4%	37.0%	32.2%	TGG	TG**A**	W202opal
e96	11.1%	23.3%	29.9%	35.6%	CGA	**T**GA	R265opal
vab-1(dx31)	50.8%	33.2%	14.0%	2.0%			
Intermediate							
e141	8.9%	14.5%	55.8%	20.7%	TGT	T**A**T	C90Y
e1208	8.8%	15.0%	51.0%	25.2%	CCG	C**T**G	P108L
Weak							
ju90	3.0%	2.6%	7.3%	87.0%	ATG	AT**A**	M1I
sy167	7.6%	8.1%	39.3%	45.0%	TTT|gtga	TTT|**a**tga	exon 3 splice donor

We classified *vab-2/efn-1* mutations as strong (>30% embryonic + larval lethality), intermediate (20%–30% lethality) or weak (<20% lethality); the *vab-1* null allele *dx31* (George et al., 1998) is included for comparison. Wild-type and mutant *vab-2/efn-1* genomic DNA sequences are shown, with the predicted effects on VAB-2/EFN-1 protein.

Mutations in the *vab-2* gene cause defects in epidermal morphogenesis like those of *vab-1* (Brenner, 1974). Examination of sequence data for the *vab-2* genomic region revealed a predicted ephrin gene; all *vab-2* alleles cause sequence alterations in this gene (Table 1), showing that this gene is *vab-2*. Four *C. elegans* ephrin (*efn*) genes have been identified (Wang et al., 1999), among which *vab-2* corresponds to *efn-1*; in this paper we will refer to this gene as *vab-2/efn-1*.

We confirmed the structure of the *vab-2/efn-1* gene (see Experimental Procedures). VAB-2/EFN-1 is most similar to vertebrate ephrins (Pandey et al., 1995). Vertebrate ephrins are GPI-anchored (ephrin-A) or transmembrane (ephrin-B) proteins. VAB-2/EFN-1 contains a predicted GPI attachment signal at its C terminus and thus is structurally similar to vertebrate ephrin-As. The conserved domain of VAB-2/EFN-1 is significantly more similar to those of ephrin-Bs than to those of ephrin-As (Figure 1C). VAB-2 thus shares features with both subfamilies of vertebrate ephrins. Five strong *vab-2/efn-1* alleles result in nonsense mutations (Table 1; Figure 1B) and are probably null mutations. Two intermediate alleles, *e141* and *e1208*, encode missense alterations (C90Y and P108L) in the receptor binding domain.

VAB-2/EFN-1 is GPI-Anchored and Binds VAB-1 with High Affinity

Vertebrate EphA receptors bind ephrin-A ligands, and EphB receptors bind ephrin-B ligands (Gale et al., 1996). VAB-1 is equally similar to the EphA and EphB receptor subfamilies (George et al., 1998). Because VAB-1 and VAB-2/EFN-1 are divergent members of their families, we asked whether they bind one another with high affinity. Full-length VAB-2/EFN-1 was expressed as a cell surface protein in 293T cells (Figure 2B). To determine whether VAB-2/EFN-1 was GPI-anchored, we incubated VAB-2/EFN-1-expressing cells with phosphatidylinositol-specific phospholipase C (PI-PLC), an enzyme that cleaves GPI anchors (Ferguson and Williams, 1988). VAB-2/EFN-1 was released into the supernatant by PI-PLC treatment (Figures 2A and 2D), showing that VAB-2/EFN-1 is GPI anchored.

To test whether VAB-2/EFN-1 binds VAB-1, we tested whether the extracellular domain of VAB-1 expressed as a soluble fusion protein with alkaline phosphatase (VAB-1-AP) could bind 293T cells expressing VAB-2/EFN-1. VAB-1-AP binding to cells expressing VAB-2/EFN-1 was detectable by staining for AP (Figures 2F and 2G) and was abolished by pretreatment with PI-PLC or with anti-VAB-2/EFN-1 antibodies (Figure 2G, and data not shown). VAB-1-AP colocalized with VAB-2 when bound to VAB-2-expressing cells (Figures 2H–2J). We measured the affinity of VAB-1-AP for VAB-2/EFN-1 in equilibrium binding experiments (Figure 2K). Specific binding curves of VAB-1-AP to cells expressing VAB-2/EFN-1 showed saturation, with a calculated K_D of 5 nM, comparable to vertebrate Eph receptor-ephrin K_Ds of 0.1–25 nM (Flanagan and Vanderhaeghen, 1998); negative controls showed lower binding and no saturation (Figure 2K). These data show that VAB-2/EFN-1 can bind VAB-1 with high affinity.

Finally, we asked whether the missense mutations caused by the *vab-2* alleles *e141* and *e1208* affected the affinity of VAB-2/EFN-1 for VAB-1. The C90Y and P108L mutant VAB-2/EFN-1 proteins were expressed at equivalent levels to wild-type VAB-2/EFN-1 (Figure 2C), and did not show specific binding to VAB-1 (Figure 2L). Thus, mutations that reduced the affinity of VAB-2/EFN-1 for VAB-1 also reduced *vab-2/efn-1* function.

vab-2/efn-1 Mutants Display Defects in Morphogenesis Similar to Those of *vab-1* Mutants

vab-2/efn-1 mutations cause variable and incompletely penetrant defects in epidermal morphogenesis (Table 1; Figure 3). We analyzed the phenotypes caused by the strong *vab-2/efn-1* allele *ju1* in detail. About 10% of *vab-2/efn-1* mutants arrested during embryonic stages; about 20% of *vab-2/efn-1* animals arrested as larvae due to defects in head and tail morphogenesis. About 50% of *vab-2/efn-1* adults displayed the "Notched-head" phenotype, resulting from aberrant morphogenesis of head epidermis (Figure 3J). The expression of

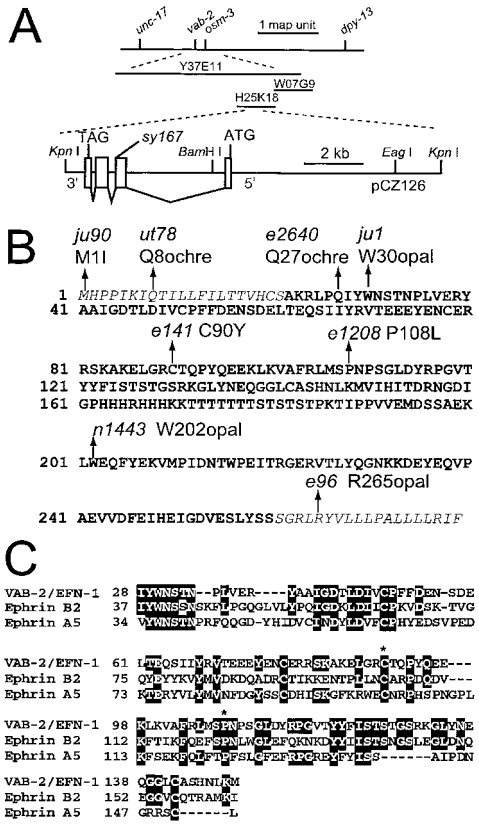

Figure 1. *vab-2* Encodes *C. elegans* Ephrin EFN-1

(A) Genetic and physical maps of the *vab-2/efn-1* locus and structure of the *vab-2/efn-1* gene. *vab-2/efn-1* maps 0.1 map units to the left of *osm-3* on LGIV. Cosmid, YAC, and fosmid clones were mapped by the *C. elegans* genome project; *vab-2/efn-1* is rescued by a 12 kb KpnI fragment (pCZ126) from fosmid H25K18, which overlaps cosmid W07G9. *vab-2/efn-1* is the predicted gene Y37E11A_93.a in the *C. elegans* genomic database. The intron–exon structure of *vab-2/efn-1* is conserved with those of vertebrate ephrin-As: the locations of the introns between exons 1, 2, and 3 are conserved between *vab-2/efn-1*, murine ephrin-A3, ephrin-A4, and human ephrin-A2 (Cerretti and Nelson, 1998).

(B) Sequence of VAB-2/EFN-1 protein, showing locations of mutations. The signal sequence (italicized) is predicted to be cleaved after residue A22. The conserved putative receptor-binding domain (residues 28–149) is followed by a spacer (residues 150 to 260). The VAB-2/EFN-1 C terminus (italicized) is hydrophobic and is predicted to be cleaved after S260.

(C) Alignment of the VAB-2/EFN-1 conserved domain with those of the most similar ephrin-A and ephrin-Bs. Conserved domains were aligned using CLUSTAL W; identities to VAB-2/EFN-1 are in black. Within this domain, VAB-2/EFN-1 is 38% identical (47/121 residues) to human ephrin-B2 (Cerretti et al., 1995) and 28% identical (34/121) to chicken ephrin-A5 (Drescher et al., 1995). Asterisks mark residues affected by *vab-2/efn-1* missense mutations.

several neuronal and epidermal marker genes was normal in *vab-2/efn-1* mutants (data not shown), suggesting that *vab-2/efn-1* is not required for cell fate specification.

To understand the role of *vab-2/efn-1* in morphogenesis, we used four-dimensional (4D) Nomarski microscopy (Thomas et al., 1996) to examine *vab-2/efn-1* mutant embryos. We found that *vab-2/efn-1* mutants, like *vab-1* mutants, were defective in two phases of embryogenesis: in the movements of neuroblasts during closure of the ventral gastrulation cleft (Figure 3A), and in epidermal enclosure (Figure 3B). Because most *vab-2/efn-1* mutants displayed phenotypes similar to those of *vab-1* mutants, we classified them using the same criteria (George et al., 1998). Twelve percent of *vab-2/efn-1* embryos displayed severe defects in gastrulation cleft closure and arrested in epidermal enclosure (class I and II phenotypes; Figures 3G and 3H). Sixteen percent of *vab-2/efn-1* embryos displayed defects in gastrulation cleft closure, underwent normal epidermal enclosure, and elongated to the 2- or 3-fold stage, when they ruptured in the head (Figure 3I); this phenotype is similar to the *vab-1* class IV phenotype. Most *vab-2/efn-1* embryos (72%) displayed mild defects in morphogenesis (class V; Figure 3J).

The phenotypes of *vab-2/efn-1* mutants were thus largely indistinguishable from those of *vab-1* mutants. The major difference was that *vab-1* null mutations caused more penetrant defects than those of strong *vab-2/efn-1* mutants (see below). *vab-2/efn-1* adults were also more frequently egg-laying defective than *vab-1* mutants. Thus, *vab-2/efn-1* mutant phenotypes were mostly overlapping with those of *vab-1* mutants, consistent with *vab-2/efn-1* and *vab-1* functioning in the same process.

VAB-2/EFN-1 Is Expressed in a Subset of Neurons during Embryogenesis, Adjacent to VAB-1-Expressing Neurons

To determine the cells in which VAB-2/EFN-1 was expressed, we made anti-VAB-2/EFN-1 antisera. These antisera detected VAB-2/EFN-1 in animals that overexpressed VAB-2/EFN-1 from rescuing transgenes, but did not detect endogenous VAB-2/EFN-1, suggesting that VAB-2/EFN-1 may be expressed at low levels. We first detected VAB-2/EFN-1 expression at the 100-cell stage in several cells in the anterior and posterior (data not shown). After gastrulation VAB-2/EFN-1 was expressed in lateral cells, corresponding to neuroblasts. During epidermal enclosure VAB-2/EFN-1 was expressed in neurons in the midanterior of the embryo, beneath the leading cells of the epidermis (Figures 4A and 4B), and in several tail neurons. At later stages VAB-2/EFN-1 was expressed in the processes of many neurons (Figure 4C), and in the pharynx. Thus, VAB-2/EFN-1 was expressed mostly in the developing nervous system and not in epidermal cells before or during epidermal enclosure.

As cell contact is necessary for ephrins to signal to Eph receptors, we asked whether VAB-1 and VAB-2/EFN-1 were expressed in adjacent cells. We constructed strains in which both VAB-2/EFN-1 and GFP-tagged VAB-1 were expressed from rescuing transgenes, and detected these proteins by staining with anti-GFP and anti-VAB-2 antibodies. During ventral enclosure, VAB-1 was expressed in head neurons anterior to the leading cells of the epidermis, and in the ventral body of the embryo (blue in Figures 4D–4F); VAB-2/EFN-1 (green) was expressed in adjacent neurons. Thus, VAB-2/EFN-1 expressing cells contact VAB-1-expressing cells during embryogenesis.

We also asked whether mutations in the VAB-1 receptor led to disorganization of VAB-2/EFN-1 expressing cells, as expected from the disorganization of neuroblasts following gastrulation in *vab-1* or *vab-2/efn-1* mutants. We found that in *vab-1(e2)* mutants the VAB-2/

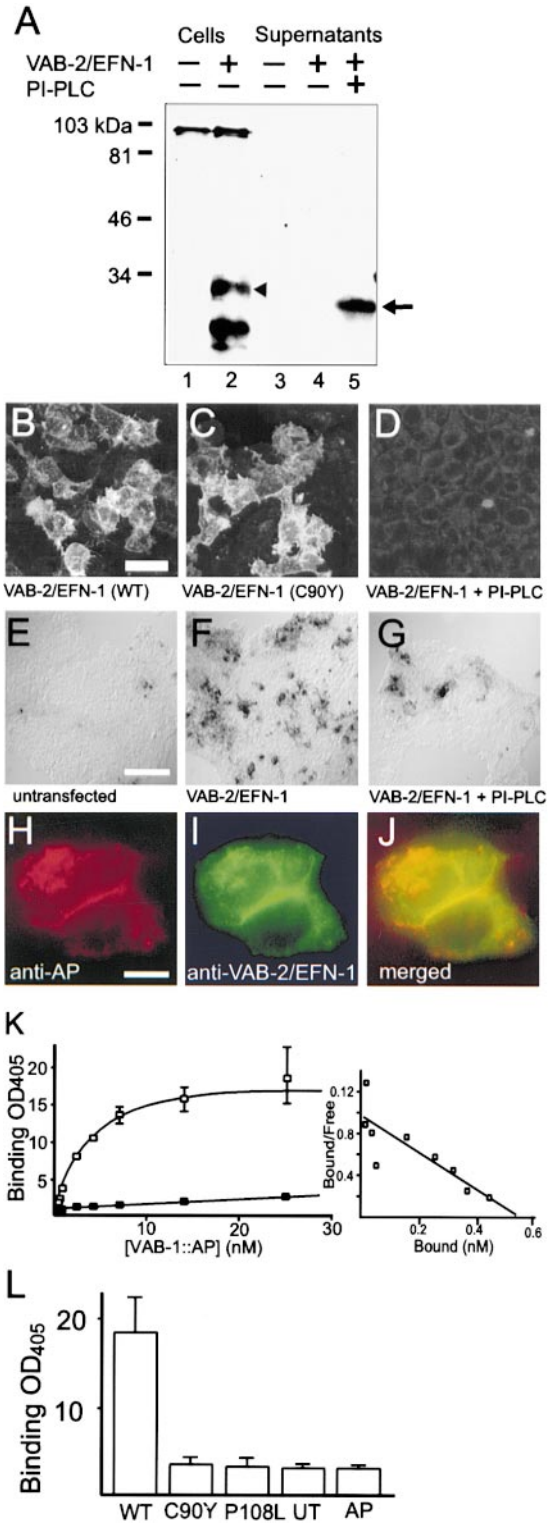

Figure 2. VAB-2/EFN-1 Is GPI-Anchored and Binds VAB-1 with High Affinity

(A) Western blot of lysates of 293T cells transiently transfected with full-length VAB-2/EFN-1, probed with anti-VAB-2/EFN-1 antisera. A 30 kDa product (arrowhead) was specific to transfected cells (lane 2), was not seen in the cell supernatant (lane 4), and likely corresponds to VAB-2/EFN-1. The predicted molecular weight of the mature VAB-2/EFN-1 peptide is 26 kDa; the difference in apparent molecular weight may reflect addition of the GPI anchor and other processing. Smaller products specific to VAB-2/EFN-1 transfected cells may be breakdown products. A single product (arrow) was detected in supernatants after treatment with PI-PLC (lane 5).

(B) Confocal image of 293T cells expressing VAB-2/EFN-1, detected with anti-VAB-2/EFN-1 antisera, showing localization to the cell surface. Bar, 20 μm (B–D).

(C) 293T cells expressing the C90Y (*e141*) mutated form of VAB-2/EFN-1, visualized as in (B), showing equivalent expression levels; similar results were obtained for the P108L (*e1208*) mutant (not shown).

(D) Anti-VAB-2/EFN-1 staining was abolished when cells expressing wild-type VAB-2/EFN-1 were pretreated with PI-PLC to cleave GPI anchors.

(E–G) VAB-1-AP specifically binds to VAB-2/EFN-1 expressing cells. Untransfected 293T cells (E) or cells transfected with VAB-2/EFN-1 (F) were incubated with 25 nM VAB-1-AP and the binding visualized using AP enzymatic activity; the interaction is sensitive to pretreatment with PI-PLC (G), or with anti-VAB-2 antisera (not shown). Bar = 150 μm.

(H–J) Colocalization of VAB-1-AP and VAB-2/EFN-1. Cells expressing VAB-2/EFN-1 were treated with VAB-1-AP, and stained with anti-AP (red) and anti-VAB-2 antibodies (green). The merged image (J) shows colocalization (yellow). Bar = 10 μm.

(K) Equilibrium binding of VAB-1-AP to VAB-2/EFN-1-transfected 293T cells (open squares) or untransfected (filled squares). Specific binding is also shown as a Scatchard plot (right). Error bars in (K) and (L) indicate standard deviations (n = 3).

(L) Mutations in the VAB-2/EFN-1 conserved domain abolish VAB-1-AP binding. Binding was measured at 25 nM VAB-1-AP, using cells expressing wild-type VAB-2/EFN-1 or the C90Y and P108L mutants. UT = untransfected. AP = secreted alkaline phosphatase binding to 293T cells expressing wild-type VAB-2/EFN-1.

EFN-1 expressing cells were frequently more spread out (Figures 4G and 4H; compare with 4A and 4B), suggesting that VAB-1 signaling prevents spreading of VAB-2-expressing cells. Spreading of VAB-2/EFN-1-expressing cells was seen in animals carrying *vab-1* null or extracellular domain alleles (*e2027, e699*; data not shown). These data suggest that epidermal defects in *vab-1* or *vab-2/efn-1* mutants may be due to disorganization of neurons.

VAB-2/EFN-1 Can Function in Neurons to Regulate Epidermal Morphogenesis

The expression pattern of VAB-2/EFN-1 suggested that, like VAB-1, it might function nonautonomously in the developing nervous system for epidermal development. We first tried to address this using genetic mosaic analysis and found that *vab-2/efn-1* was required in several lineages that generate both epidermis and neurons (data not shown). However, late losses of *vab-2/efn-1* function in neural precursors did not cause Vab phenotypes, probably because the Vab-2 phenotype is weak. We therefore asked whether neuronal expression of VAB-2/EFN-1 was sufficient to suppress the epidermal defects of *vab-2/efn-1* mutants. The *unc-119* gene is expressed in all neuronal precursors and neurons (Maduro and Pilgrim, 1995). We generated animals in which VAB-2/EFN-1 was expressed under the control of the *unc-119* promoter, and found that this panneural expression of VAB-2/EFN-1 was able to partially suppress epidermal morphology and lethal defects of *vab-2/efn-1* mutants (Figures 5A and 5B, black bars). The partial rescue may be because panneural expression of VAB-2/EFN-1 did

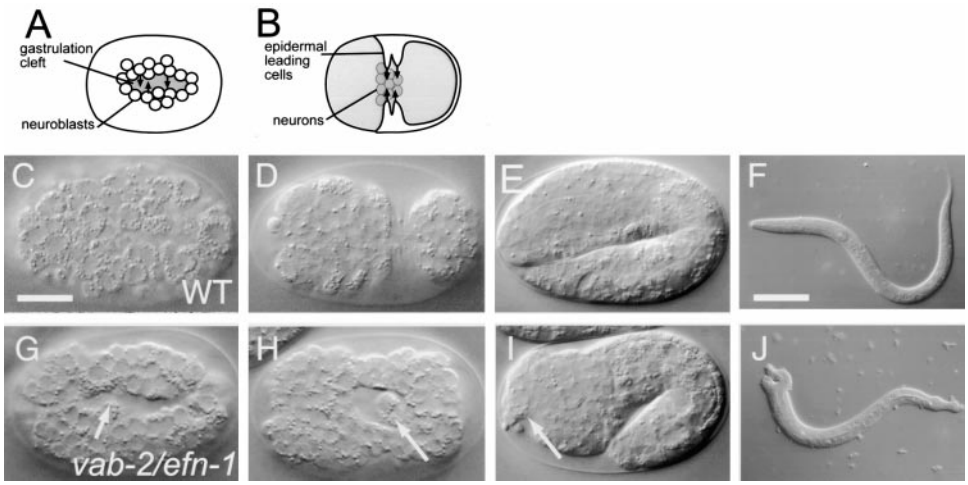

Figure 3. *vab-2/efn-1* Mutants Are Defective in Gastrulation Cleft Closure and Epidermal Enclosure

(A) Schematic of gastrulation cleft closure, ventral view.

(B) Schematic of epidermal enclosure, ventral view.

(C–F) Morphogenesis of wild-type embryos. (C) Between 230 and 290 min postfertilization, the ventral cleft following gastrulation closes. (D) Between 310 and 360 min postfertilization, the epidermis encloses ventrally. (E) Wild-type 2-fold embryo, lateral view, dorsal up. (F) Wild-type first larval stage (L1). Bar, 10 μm (C–E and G–I), 20 μm (F and J). Anterior is to the left in all panels; ventral views (C, D, G, and H) or lateral views (E, F, I, and J).

(G–J) Morphogenesis of *vab-2/efn-1(ju1)* embryos. (G) Gastrulation cleft of class I *vab-2/efn-1(ju1)* embryo. 8% (4/50) of *vab-2/efn-1* embryos displayed a class I phenotype (cf. 14% of *vab-1* embryos). Two early gastrulation clefts formed a single deep cleft (arrow) that persisted until epidermal enclosure (H); epidermal cells failed to migrate past the equator of the embryo. 4% (2/50) of animals displayed a class II phenotype, which is similar to class I but slightly weaker. (I) Rupture of head epidermis in *vab-2/efn-1(ju1)* class IV embryo, 1.5-fold stage. 16% (8/50) of *vab-2* embryos displayed a class IV phenotype, in which the gastrulation cleft was larger than normal yet closed up properly; embryos underwent epidermal enclosure and elongated to 2-fold or 3-fold stages, then ruptured in the head region (arrow). (J) Abnormal morphogenesis of head and tail epidermis in a class V *vab-2/efn-1(ju1)* L1 animal; 66% (33/50) of animals displayed a class V phenotype, in which cleft closure was normal and the epidermis closed fully. In some class V embryos the epidermis was malformed, leading to the Notch head phenotype in larvae; in 6% (3/50) of embryos the cleft was deeper than normal, and the embryo developed to hatching.

not exactly mimic the wild-type VAB-2/EFN-1 expression pattern. In contrast, epidermal expression of VAB-2/EFN-1 did not significantly rescue Vab-2 phenotypes (Figures 5A and 5B). These data suggest that VAB-2/EFN-1 can function nonautonomously in neurons to control epidermal development.

vab-2/efn-1 Mutations Synergize with *vab-1* (Kinase) Mutations

To address whether VAB-2/EFN-1 acts as a ligand for VAB-1 in vivo, we used double mutant analysis to ask if *vab-1* and *vab-2/efn-1* affect a single pathway. If *vab-2/efn-1* and *vab-1* mutations affect a single pathway, then the phenotype of a *vab-1* null mutant [*vab-1(0)*] should not be enhanced by a *vab-2/efn-1* null mutation [*vab-2/efn-1(0)*]. We found that the phenotypes of nine *vab-1(0); vab-2/efn-1(0)* strains resembled those of *vab-1(0)* strains (Figure 6A). The embryonic phenotypes of the double mutants were indistinguishable from those of *vab-1(0)* mutants, as judged by 4D analysis (data not shown). Although most double mutant strains showed a slight increase in lethality, this was significant in only four of nine strains (Figure 6A). These data suggest that *vab-2/efn-1* functions mainly in the same pathway as *vab-1*.

Mutations that disrupt the kinase domain of VAB-1 [*vab-1(k)*] do not eliminate *vab-1* function, suggesting that VAB-1 has both kinase-dependent and kinase-independent functions (George et al., 1998). As VAB-2/EFN-1 is a GPI-anchored ephrin, we predicted that it would mediate the kinase-dependent function of VAB-1, and thus *vab-2/efn-1* mutations should not show interactions with *vab-1(k)* mutations. Surprisingly, *vab-2/efn-1; vab-1(k)* double mutants showed a dramatic enhancement of Vab-1 phenotypes, and resembled *vab-1(0)* strains in phenotype and penetrance (Figure 6B). Thus, *vab-2/efn-1* mutations synergized strongly with *vab-1(k)* mutations, although not with *vab-1(0)* mutations, suggesting that *vab-2/efn-1* does not solely act in the *vab-1* kinase-dependent pathway.

We therefore asked if *vab-2/efn-1* functions in a pathway affected by mutations in the VAB-1 extracellular domain. The *vab-1* mutation *e699* encodes a missense alteration in the ligand-binding domain of VAB-1 (Himanen et al., 1998). We found that *vab-1(e699)* did not synergize strongly with *vab-2/efn-1(0)* mutations (Figure 6B). While the *e699* mutation alone causes a stronger phenotype than *vab-1(k)* alleles, the *vab-1(e699); vab-2/efn-1(0)* double mutants were significantly weaker than *vab-1(k); vab-2/efn-1(0)* double mutants. Thus, *vab-2/efn-1(0)* mutations specifically synergized with kinase domain alleles of *vab-1* and not with a more severe extracellular domain mutation. *vab-2/efn-1* might therefore act in a kinase-independent pathway that is also affected by the *vab-1(e699)* mutation.

Discussion

We previously reported that *vab-1* encodes a *C. elegans* Eph receptor tyrosine kinase that is required in neurons for normal neural and epidermal morphogenesis. Here

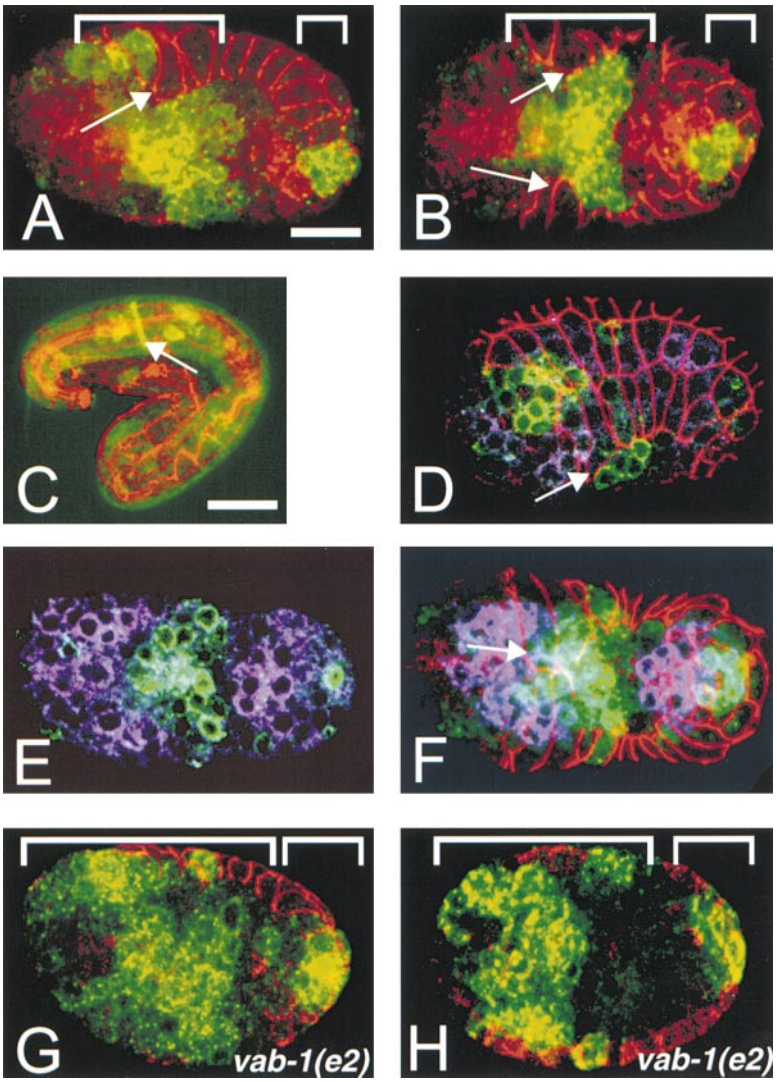

Figure 4. VAB-2/EFN-1 Is Expressed in Neurons Adjacent to VAB-1-Expressing Cells

Confocal images of VAB-2/EFN-1 expression from the *juIs53* [*vab-2/efn-1(+)*] transgene, visualized using anti-VAB-2/EFN-1 antibodies (green); epidermal adherens junctions were visualized using the MH27 monoclonal antibody (red); VAB-1::GFP expression in (D)–(F) visualized with anti-GFP antibodies (blue). Bar, 10 μm (A, B, D–H), 20 μm (C).

(A and B) Ventrolateral and ventral views of early enclosure. During epidermal enclosure VAB-2/EFN-1 is expressed in many neurons in the anterior and in several in the tail. Based on double staining with the epidermal markers MH27 and LIN-26, VAB-2/EFN-1 is not expressed in epidermal cells or precursors. Leading epidermal cells (arrows) appear to migrate directly over VAB-2/EFN-1-expressing neurons.

(C) Late embryo, 3-fold stage; the nerve ring (arrowed), head neurons, and dorsal and ventral nerve cords express VAB-2/EFN-1. Strong expression is also seen in the metacorpus, isthmus, and valve regions of the pharynx.

(D) Triple label immunofluorescence (confocal section) showing VAB-2/EFN-1 (green), VAB-1::GFP (blue), and MH27 (red). Lateral view during early enclosure; leading edges of epidermal cells are arrowed.

(E and F) VAB-2/EFN-1 and VAB-1::GFP expression after leading cells have met at the ventral midline (arrow). Ventral views; (E) is a confocal section showing only VAB-2/EFN-1 and VAB-1::GFP channels; (F) is a confocal projection of the ventral half of the embryo in all three channels. VAB-1::GFP and VAB-2/EFN-1 expressing cells form distinct, adjacent populations.

(G and H) VAB-2/EFN-1 expression in *vab-1(e2)* mutant embryos. VAB-2/EFN-1-expressing cells become more spread out, compare brackets showing extent of VAB-2/EFN-1 staining in (A) and (B) versus (G) and (H). Spreading of VAB-2/EFN-1-expressing cells was seen in 70% (135/192) of *vab-1(e2)* embryos. Mild spreading was seen in 33% (12/36) of control *juIs53* embryos.

we show that VAB-2/EFN-1 is a GPI-anchored ephrin ligand for VAB-1, and that VAB-2/EFN-1 is predominantly expressed in neurons. The epidermal defects in *vab-2/efn-1* mutants can be suppressed by neuronal but not epidermal expression of VAB-2/EFN-1. Our data support a model in which signaling between neurons is required nonautonomously for *C. elegans* epidermal development.

VAB-2/EFN-1 is a *C. elegans* Ephrin Similar to Both GPI-Linked and Transmembrane Ephrins

VAB-2/EFN-1 is a member of the ephrin family of ligands for Eph receptors. Ligands for Eph receptors were identified by expression cloning (Bartley et al., 1994; Cheng and Flanagan, 1994; Davis et al., 1994), and in assays for proteins involved in axon guidance (Drescher et al., 1995). Ephrins have previously been reported in vertebrates; our data show that, like their receptors, ephrins are likely to be conserved amongst all metazoans. Vertebrate ephrins are GPI anchored (ephrin-As) or transmembrane (ephrin-Bs) proteins. VAB-2/EFN-1 is GPI anchored and thus structurally like vertebrate ephrin-As. However, the conserved domain of VAB-2/EFN-1 resembles those of vertebrate ephrin-Bs in sequence. Thus, VAB-2/EFN-1 is an unusual ephrin and might resemble a common ancestor of the two vertebrate subclasses. Other *C. elegans* ephrins (Wang et al., 1999), like VAB-2/EFN-1, are predicted to be GPI anchored with conserved domains more similar to those of ephrin-Bs. The *C. elegans* genome sequence encodes one Eph receptor, VAB-1, suggesting that all four worm ephrins might interact with the VAB-1 receptor.

VAB-2/EFN-1 May Partly Function in a VAB-1 Kinase-Independent Pathway

Mutations that disrupt the kinase domain of VAB-1 cause weak mutant phenotypes, suggesting that VAB-1

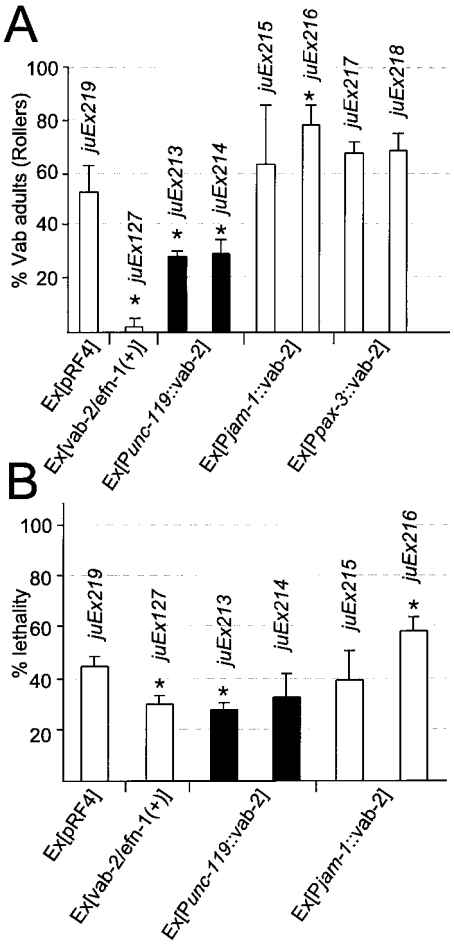

Figure 5. Neuronal VAB-2/EFN-1 Can Suppress Epidermal Defects of *vab-2/efn-1* Mutants

Extrachromosomal arrays expressing VAB-2/EFN-1 in neurons (P*unc-119*::VAB-2/EFN-1), epidermal cells (P*pax-3*::VAB-2/EFN-1), or all epithelial cells (P*jam-1*::VAB-2/EFN-1) were crossed into *vab-2/efn-1(ju1)* backgrounds. At least three broods were scored for each genotype; adult roller animals were scored for the Vab epidermal phenotype. Error bars indicate standard deviations ($n \geq 3$). Asterisks indicate significant differences (Student's t test, $p = 0.05$) from negative control lines bearing the pRF4 array (*juEx219*) alone. The rescuing *vab-2/efn-1* array *juEx127* is included as a positive control.

(A) Percentage of adult rollers in *vab-2/efn-1(ju1)* backgrounds that displayed the Vab epidermal phenotype. The P*unc-119*::VAB-2/EFN-1 arrays displayed significant rescue; the P*pax-3*::VAB-2/EFN-1 and P*jam-1*::VAB-2/EFN-1 arrays did not show rescuing activity.

(B) Percentage lethality in *vab-2/efn-1(ju1)* transgenic lines. Lethality was reduced in both P*unc-119*::VAB-2/EFN-1 lines; the reduction was significant in only one line.

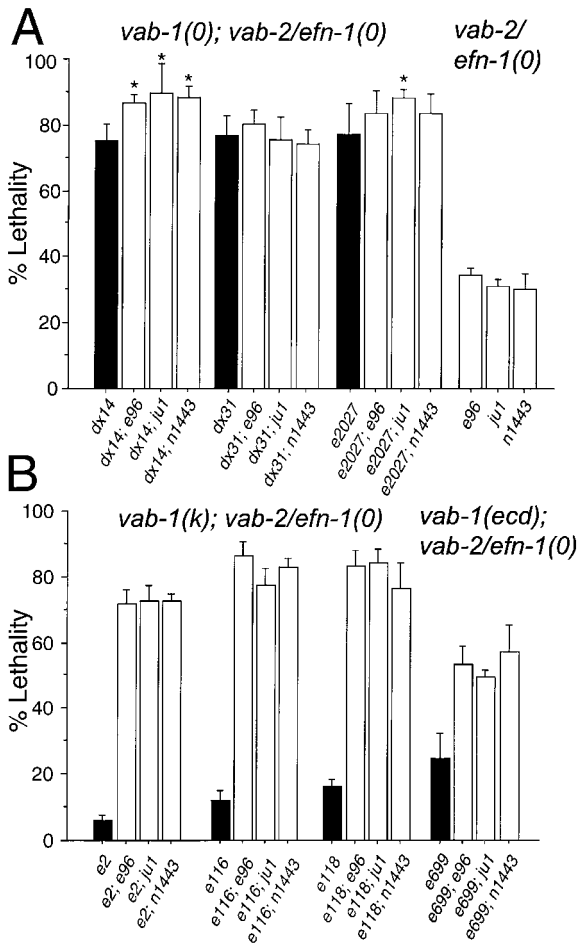

Figure 6. Double Mutant Analysis of *vab-1* and *vab-2/efn-1*

(A) Analysis of strains doubly mutant for *vab-1* null mutations (*dx14*, *dx31*, or *e2027*) and for *vab-2/efn-1* null mutations (*e96*, *ju1,* or *n1443*). Error bars indicate standard deviations. Double mutant strains marked * were significantly more penetrant ($p = 0.05$) than the corresponding *vab-1* single mutant.

(B) Analysis of strains doubly mutant for *vab-1* kinase domain mutations (*e2*, *e116*, or *e118*), the *vab-1* extracellular domain allele *e699*, and *vab-2/efn-1* null mutations.

has both kinase-dependent and kinase-independent functions. As VAB-2/EFN-1 is a GPI-linked ephrin, we expected that VAB-2/EFN-1 would only function to activate the VAB-1 kinase, and thus genetically should be in the same pathway as *vab-1* kinase mutations. Strikingly, *vab-2/efn-1* mutations synergized strongly with *vab-1(k)* mutations. Mutations that show synergistic enhancement may affect redundant pathways (Guarente, 1993). *vab-2/efn-1* mutations did not synergize with a *vab-1* extracellular domain mutation, showing that the synergism is specific to kinase domain alleles of VAB-1. These data suggest that some or all of VAB-2/EFN-1's functions may be in a VAB-1 kinase-independent pathway.

There are several possible ways in which GPI-linked ephrins such as VAB-2/EFN-1 could function in kinase-independent pathways. First, VAB-1 and VAB-2/EFN-1 might act as cell adhesion molecules, independent of signaling activity. Second, analogous to the signaling functions of transmembrane ephrins, VAB-2/EFN-1 could mediate a "reverse" signal, via mechanisms known for other GPI-linked proteins: VAB-2/EFN-1 might associate with transmembrane coreceptors, as shown for the CNTF receptor (Davis et al., 1991), or it could localize to membrane rafts, allowing a signal to be transduced to the VAB-2/EFN-1-expressing cell (Simons and Ikonen, 1997; Thomas and Brugge, 1997). Recent work suggests that EphA receptors have nonautonomous effects, suggesting that vertebrate ephrin-As might also transduce reverse signals (Araujo et al., 1998). Finally, the kinase-independent function of VAB-1 need not involve reverse signaling: ligands could signal via the

VAB-1 cytoplasmic domain in a way that does not involve VAB-1 kinase activity. Ephrins can activate Eph receptors in multiple ways that do not correlate with receptor phosphorylation (Stein et al., 1998), although all known intracellular responses of Eph receptors require an active kinase. Further study of the VAB-2/EFN-1 pathway may distinguish these possibilities.

Signaling within the Developing Nervous System Is Required for *C. elegans* Epidermal Morphogenesis

The VAB-1 Eph receptor is required in neurons for epidermal morphogenesis. How might lack of VAB-1 in neurons cause defects in the epidermis? We proposed two models for this nonautonomy of VAB-1 (George et al., 1998): the "steric hindrance" model and the "reverse signaling" model; these models are not mutually exclusive. In the steric hindrance model, VAB-1 signaling operates between neuroblasts and neurons, and lack of VAB-1 causes neurons to be disorganized; enclosure is defective because the epidermal cells cannot move over the abnormal neuronal substrate. In the reverse signal model, VAB-1 signals directly from neurons to the epidermal cells; in *vab-1* mutants such cues are absent and epidermal cells fail to migrate normally.

Our analysis of *vab-2/efn-1* supports a steric hindrance model for the nonautonomous role of ephrin signaling. VAB-2/EFN-1 is mostly expressed in neuroblasts or neurons, and neuron-specific expression of VAB-2/EFN-1 can partly rescue epidermal defects of *vab-2/efn-1* mutants, showing that VAB-2/EFN-1 can function in neurons to regulate epidermal development. Furthermore, mutations in the VAB-1 receptor cause disorganization of the VAB-2/EFN-1-expressing neurons. The spreading of VAB-2/EFN-1-expressing cells in *vab-1* mutants likely reflects abnormal cell migration or adhesion, as *vab-1* mutants do not display cell fate transformations. This role of VAB-1 in preventing cell spreading is strikingly reminiscent of the cell sorting functions of Eph signaling in vertebrate neurogenesis (Mellitzer et al., 1999; Xu et al., 1999).

We conclude that VAB-2/EFN-1 signaling to VAB-1 occurs between neuronal precursors, and regulates cell adhesion or movement. In the absence of VAB-1 or VAB-2/EFN-1, neuroblasts fail to close up the ventral gastrulation cleft and as a result, descendant neurons are disorganized. Disorganized neurons might block epidermal movements directly (true "steric hindrance") or indirectly: for example, the boundary between VAB-1 and VAB-2/EFN-1-expressing cells might attract migrating epidermal cells; if this boundary is disorganized, epidermal migrations would be disrupted. An analogous situation might occur in vertebrate angiogenesis, where ephrin signaling between endocardial cells is required for the development of overlying myocardial trabeculae (Wang et al., 1998). Such models do not rule out signaling from neurons to epidermis, possibly via other ephrins; however, of the three other *C. elegans* ephrins, at least two are expressed mainly in neurons (Wang et al., 1999, and our unpublished data). The small number of Eph receptors and ephrins in *C. elegans* suggests that it will be feasible to dissect the complete network of Eph/ephrin signaling in a simple animal.

Experimental Procedures

Genetic Analysis

C. elegans worms were cultured as described by Brenner (1974) at 20°C unless noted. Mutations used were: LGII: *vab-1(e2, e116, e118, dx14, dx31, e2027)*; LGIV: *unc-17(e113), dpy-13(e184*sd); LGX: *lin-15(n765*ts). Mutations are described in George et al. (1998) or Hodgkin (1997). *vab-2/efn-1* alleles were isolated by S. Brenner (*e96, e141*), J. Hodgkin (*e1208*), S. Ahmed (*e2640*), Y. Jin (*ju1*), M. Ding (*ju90*), L. Bloom (*n1443*), H. Chamberlin (*sy167*), and I. Katsura (*ut78*). All *vab-2/efn-1* alleles were induced after ethylmethanesulfonate mutagenesis. The strong *vab-2/efn-1* alleles *e96*, *n1443*, and *ju1* behave as recessive zygotic mutations (data not shown). Map data are available from the *Caenorhabditis* Genetics Center. Penetrance of Vab-2 mutant phenotypes was quantitated as described (George et al., 1998). Three to seven broods were scored for each genotype in Table 1 and Figure 6.

vab-1; vab-2 double mutants were constructed using *dpy-13*(*e184*sd) as a dominant marker in *trans* to *vab-2*. *vab-2/unc-17 dpy-13* heterozygous males were mated with *vab-1; unc-17 dpy-13* hermaphrodites, and semi-Dpy (*vab-1/+; unc-17 dpy-13/vab-2*) F_1 cross progeny were picked. Vab semi-Dpy F_2 animals were picked, and Vab non-Dpy F_3 animals were picked from their progeny, of putative genotype *vab-1; vab-2*. Homozygosity for both mutations was confirmed by complementation tests. We analyzed differences in lethality using one-way Anova (Statview). Significance was evaluated using the Fisher PLSD post hoc test with a significance level of $p = 0.05$.

Four-Dimensional Microscopy

We made 4D movies using a Zeiss Axioskop with Z axis drive and shutter (Ludl Electronic Products). Images were collected with a Dage-MTI VE1000 CCD camera, digitized with a Scion AG-5 frame grabber, converted to Quicktime movies and played using 4-D Grabber and 4-D Viewer software (C. Thomas, University of Wisconsin, Madison). To make movies we recorded 30 focal planes 0.5 μm apart, every 60 s from early gastrulation (~100 min postfertilization) until the embryo had reached a terminal phenotype. We recorded movies from 50 *vab-2(ju1)* embryos. Fourteen of these 50 embryos arrested in embryogenesis; the difference in penetrance from that observed in brood counts probably reflects the small sample size, as 100% of control embryos hatched under our conditions.

Cloning and Molecular Analysis of *vab-2/efn-1*

We identified an ephrin gene in sequence of the YAC clone Y37E11. A genomic fosmid clone, H25K18, that contains the *vab-2/efn-1* gene was identified by Stephanie Chissoe (*C. elegans* Genome Consortium). We subcloned a 12.8 kb KpnI fragment of H25K18 into pBluescript to create the clone pCZ126 (Figure 1). *vab-2/efn-1(e96)* hermaphrodites were transformed with pCZ126 (30 μg/ml) and pRF4 (30 μg/ml), which confers a roller phenotype, using standard methods (Mello et al., 1991). Transgenic lines were established from transformed F_2 animals. 3/3 lines (arrays *juEx127*, *juEx128*, *juEx129*) showed rescue of adult Vab phenotypes (2.2% of RoIs were Vab, $n = 498$) compared to control lines bearing pRF4 alone (66.1% of RoIs were Vab, $n = 168$). An integrated version of *juEx127*, *juIs53*, was isolated after X-ray mutagenesis, and rescued the lethality of *vab-2/efn-1(e96)* (1.6% lethality, $n = 303$; 0.5% Vab, $n = 727$).

We used RT-PCR to generate cDNAs containing the predicted *vab-2/efn-1* open reading frame; the resulting clone (pCZ36) was sequenced. We found no evidence for alternative processing of the *vab-2/efn-1* message from RT-PCR experiments. The *vab-2/efn-1* cDNA sequence contains an 837 bp open reading frame, and a 3′ UTR of ~170 bp. We detected a *vab-2/efn-1* transcript of ~1.2 kb using Northern blots of total *C. elegans* RNA (data not shown), consistent with our cDNA analysis. We determined the sequences of *vab-2/efn-1* mutant genomic DNAs as described (George et al., 1998).

Neuronal- and Epidermal-Specific VAB-2/EFN-1 Constructs

We amplified the *vab-2/efn-1* coding sequence using PCR and cloned it into the *unc-119* promoter vector pBY103 (Maduro and Pilgrim, 1995) using the BamHI and MscI sites. Epidermal specific

vab-2/efn-1 constructs were made by replacing the *unc-119* promoter with a *pax-3* (F27E5.2) promoter or a *jam-1* promoter. The *pax-3* promoter is contained in the 3.2 kb BamHI-EcoRV fragment of cosmid F27E5, and is expressed in embryonic epidermal cells (A. D. C., unpublished results). *jam-1* encodes the MH27 antigen, expressed in all epithelial cells but not in neurons (Mohler et al., 1998). Details of plasmid constructions are available on request.

Transgenic lines bearing the above constructs injected at high concentrations (>30 ng/μl) frequently displayed lethality and morphogenetic defects. For rescue tests we reduced the concentration of the constructs to levels that caused <5% abnormal phenotypes in a *vab-2/efn-1(+)* background, with the exception of the P*pax-3*::VAB-2/EFN-1 arrays, which cause 15%–20% Vab phenotypes in adults. P*unc-119*::VAB-2/EFN-1 was injected at 15 ng/μl (arrays *juEx213*, *juEx214*); P*pax-3*::VAB-2/EFN-1 was injected at 30 ng/μl (arrays *juEx215*, *juEx216*); P*jam-1*::VAB-2/EFN-1 was injected at 10 ng/μl (arrays *juEx217*, *juEx218*). All constructs were injected with pRF4 at 30 ng/μl. Transgenic arrays transmitting to 30%–40% of progeny were crossed into a *vab-2/efn-1(ju1)* background and rescue of Vab-2 phenotypes scored in blind tests.

VAB-2/EFN-1 Antibody Production and *C. elegans* Immunocytochemistry

To express VAB-2/EFN-1 in bacteria we cloned residues 27 to 240 of VAB-2/EFN-1 into pGEX4T3 (Pharmacia). GST-VAB-2 fusion proteins were induced in *E. coli* TG1 cells, purified by SDS-PAGE, and injected into rabbits. Anti-GST-VAB-2 antisera were preabsorbed by incubation with protein acetone powders derived from 293T cells, *E. coli*, and *vab-2(ju1)* worms, and by binding to a GST-VAB-2/EFN-1 Affigel-15 (BioRad) column, followed by extensive washing and elution.

To stain *C. elegans* embryos, we fixed the embryos in methanol and 2% paraformaldehyde and permeabilized them by freeze-thawing (Finney and Ruvkun, 1990). Data were collected from strain CZ1002 [*vab-2/efn-1(e96) juIs53*]. Affinity purified anti-VAB-2/EFN-1 antisera were used at 1:200 dilution; MH27 monoclonals (Francis and Waterston, 1991) were used at 1:1500 dilution. Fluorescently conjugated secondary antibodies were used at 1:200 to 1:500 dilution and data collected on a Leica TCS-NT confocal microscope. In double and triple staining experiments we used animals bearing the VAB-1::GFP arrays *juIs32* or *juIs33* and the VAB-2/EFN-1 array *juIs53*. To detect VAB-1::GFP, we used chicken anti-GFP polyclonal antibodies (Chemicon) at 1:200 dilution, visualized using donkey anti-chicken IgG secondary antibodies conjugated to Cy3 or Texas Red (Jackson).

Mammalian Cell Culture

To express full-length VAB-2/EFN-1, we cloned a VAB-2/EFN-1 cDNA into the BamHI and XhoI sites of pcDNA1 (Invitrogen), creating pCZ138. A construct encoding a soluble VAB-1-AP fusion protein was made by amplifying the entire VAB-1 extracellular domain (residues 1–549) using PCR from a *vab-1* cDNA; this fragment was cloned into the HindIII site of APtag2 creating pCZ144. To express soluble AP alone, we transfected cells with the APtag4 vector (Cheng et al., 1995).

293T cells were obtained from Z. He and M. Tessier-Lavigne (UCSF). Cells at 40%–60% confluence were transiently transfected with 4 μg DNA using LipofectAMINE (GIBCO-BRL) in 25 cm^2 tissue culture flasks (Corning) or 6-well plates (Falcon). For soluble VAB-1-AP fusions, the supernatant was collected 48 hr post transfection for 3 days. Supernatants were either used directly or were concentrated using Centricon 30 concentrators (Amicon), and diluted to 0.2–25 nM in DMEM without serum (Fisher), using the formula 36 OD_{405}/hr = 1 pmol VAB-1-AP (Cheng and Flanagan, 1994). Cells expressing full-length VAB-2/EFN-1 were used 48 hr posttransfection. Binding experiments were performed as described (Flanagan and Leder, 1990; Cheng and Flanagan, 1994), in triplicate for each concentration. To determine GPI anchorage, cells were treated with 250 mU/ml phosphatidylinositol-specific phospholipase C (Sigma) in complete medium for 2 hr at 37°C.

To detect VAB-2/EFN-1 on the surface of 293T cells, cells expressing VAB-2/EFN-1 were washed in DMEM and incubated with anti-VAB-2/EFN-1 antisera (1:1000) in DMEM for 1 hr at room temperature. Cells were washed with 10 vol DMEM and fixed with ice cold 65% acetone, 8% formalin in 20 mM HEPES pH 7.0, for 20 min at −20°C. Cells were washed 3 times with HBAH buffer (Hank's balanced salt solution, 0.5 mg/ml BSA, 0.1% NaN_3, 20 mM HEPES, pH 7.0. FITC-conjugated goat anti-rabbit antisera (Cappel) were used at 1:500 dilution in buffer A (Finney and Ruvkun, 1990), and incubated at room temperature for 1 hr. Cells were washed in 6× 1 ml buffer B and stored in 70% glycerol and 10% DABCO (1,4-diazobicyclo-[2.2.2]-octane) (Aldrich). To show colocalization of VAB-1-AP binding and VAB-2/EFN-1, VAB-1-AP (900 ng/ml) was bound to VAB-2/EFN-1 expressing cells in complete medium for 1 hr at 37°C. Cells were washed and fixed as above. VAB-1-AP was detected by anti-AP monoclonals (Genzyme) at 1:1000 dilution, and VAB-2/EFN-1 detected by anti-VAB-2/EFN-1 antisera (1:500). Primary antibodies were incubated for 2 hr to overnight at room temperature, and staining visualized using appropriate secondary antibodies.

For the Western blot analysis of VAB-2/EFN-1, cells from a 25 cm^2 flask of confluent cells were washed off, spun (150 μl pellets) and resuspended in 1 ml 2× sample buffer, boiled, and 20 μl loaded onto a 15% acrylamide gel, subjected to SDS-PAGE, and electroblotted onto nitrocellulose. Anti-VAB-2/EFN-1 was used at 1:1000 dilution. Anti-rabbit HRP-conjugated antibodies (Amersham) were used at 1:5000 dilution and detected using Super Signal (Pierce).

To generate mutant forms of VAB-2/EFN-1 in pcDNA1, we designed primers containing the missense mutations in *e141* and *e1208* and used these primers in PCRs. First, two PCRs were carried out using *vab-2/efn-1* cDNA as template: one, using a 5′ sense primer specific for *vab-2/efn-1* and the antisense primer of the complementary mutated primer; and two, using the sense primer of the complementary mutated primer and a 3′ anti-sense primer specific for *vab-2/efn-1*. The two PCR products were pooled and used as templates in a third PCR using the original 5′ and 3′ *vab-2/efn-1* primers to generate a *vab-2/efn-1* cDNA containing the desired mutation. Clones were confirmed by sequencing.

Acknowledgments

We thank the colleagues above for *vab-2/efn-1* alleles, the *C. elegans* Genome Consortium for sequence data, and Stephanie Chissoe for H25K18. We thank Chuck Wilson for cell culture facilities, Inessa Grinberg for sequencing *e2640*, Bill Rice for statistical advice, and members of the Chisholm and Jin labs for help and encouragement. We thank Andy Fire for *C. elegans* vectors, John Flanagan for APtag vectors, and Charles Thomas for 4D software. We thank Renee Baran, Lindsay Hinck, Yishi Jin, Andrew Spence, and John Tamkun for comments concerning the manuscript. We especially thank Jeff Simske and Jeff Hardin for the *jam-1* promoter, and Xiangmin Wang, Tony Pawson, and Joe Culotti for communication of unpublished results. This work was supported by a Human Frontiers Science Program Postdoctoral Fellowship (I. D. C.-S.), a University of California Biotechnology training grant (S. E. G.), and grants to A. D. C. from the University of California CRCC and the NIH (R01 GM54657). A. D. C. is an Alfred P. Sloan Foundation Research Fellow.

Received February 10, 1999; revised November 9, 1999.

References

Araujo, M., Piedra, M.E., Herrera, M.T., Ros, M.A., and Nieto, M.A. (1998). The expression and regulation of chick *EphA7* suggests roles in limb patterning and innervation. Development *125*, 4195–4204.

Bard, J. (1992). Morphogenesis (Cambridge, UK: Cambridge University Press).

Bartley, T.D., Hunt, R.W., Welcher, A.A., Boyle, W.J., Parker, V.P., Lindberg, R.A., Lu, H.S., Colombero, A.M., Elliott, R.L., Guthrie, B.A., et al. (1994). B61 is a ligand for the ECK receptor protein-tyrosine kinase. Nature *368*, 558–560.

Brenner, S. (1974). The genetics of *Caenorhabditis elegans*. Genetics *77*, 71–94.

Brückner, K., Pasquale, E.B., and Klein, R. (1997). Tyrosine phosphorylation of transmembrane ligands for Eph receptors. Science *275*, 1640–1643.

Cerretti, D.P., Vanden Bos, T., Nelson, N., Kozlosky, C.J., Reddy, P., Maraskovsky, E., Park, L.S., Lyman, S.D., Copeland, N.G., Gilbert,

D.J., et al. (1995). Isolation of LERK-5: a ligand of the eph-related receptor tyrosine kinases. Mol. Immunol. *32*, 1197–1205.

Cerretti, D.P., and Nelson, N. (1998). Characterization of the genes for mouse LERK-3/Ephrin-A3 (*Epl3*), mouse LERK-4/Ephrin-A4 (*Epl4*), and human LERK-6/Ephrin-A2 (*EPLG6*): conservation of intron/exon structure. Genomics *47*, 131–135.

Cheng, H.J., and Flanagan, J.G. (1994). Identification and cloning of ELF-1, a developmentally expressed ligand for the Mek4 and Sek receptor tyrosine kinases. Cell *79*, 157–168.

Cheng, H.-J., Nakamoto, M., Bergemann, A.D., and Flanagan, J.G. (1995). Complementary gradients in expression and binding of ELF-1 and Mek4 in development of the topographic retinotectal projection map. Cell *82*, 371–381.

Conway, G., Margoliath, A., Wong-Madden, S., Roberts, R.J., and Gilbert, W. (1997). Jak1 kinase is required for cell migrations and anterior specification in zebrafish embryos. Proc. Natl. Acad. Sci. USA *94*, 3082–3087.

Costa, M., Raich, W., Agbunag, C., Leung, B., Hardin, J., and Priess, J.R. (1998). A putative catenin-cadherin system mediates morphogenesis of the *Caenorhabditis elegans* embryo. J. Cell Biol. *141*, 297–308.

Davis, S., Aldrich, T.H., Valenzuela, D.M., Wong, V.V., Furth, M.E., Squinto, S.P., and Yancopoulos, G.D. (1991). The receptor for ciliary neurotrophic factor. Science *253*, 59–63.

Davis, S., Gale, N.W., Aldrich, T.H., Maisonpierre, P.C., Lhotak, V., Pawson, T., Goldfarb, M., and Yancopoulos, G.D. (1994). Ligands for the EPH-related receptor tyrosine kinases that require membrane attachment or clustering for activity. Science *266*, 816–819.

Drescher, U., Kremoser, C., Handwerker, C., Loschinger, J., Noda, M., and Bonhoeffer, F. (1995). In vitro guidance of retinal ganglion cell axons by RAGS, a 25 kDa tectal protein related to ligands for Eph receptor tyrosine kinases. Cell *82*, 359–370.

Ferguson, M.A., and Williams, A.F. (1988). Cell-surface anchoring of proteins via glycosyl-phosphatidylinositol structures. Annu. Rev. Biochem. *57*, 285–320.

Finney, M., and Ruvkun, G. (1990). The *unc-86* gene product couples cell lineage and cell identity in C. elegans. Cell *63*, 895–905.

Flanagan, J.G., and Leder, P. (1990). The kit ligand: a cell surface molecule altered in steel mutant fibroblasts. Cell *63*, 185–194.

Flanagan, J.G., and Vanderhaeghen, P. (1998). The ephrins and Eph receptors in neural development. Annu. Rev. Neurosci. *21*, 309–345.

Francis, G.R., and Waterston, R.H. (1991). Muscle cell attachment in *Caenorhabditis elegans*. J. Cell Biol. *114*, 465–479.

Gale, N.W., Holland, S.J., Valenzuela, D.M., Flenniken, A., Pan, L., Ryan, T.E., Henkemeyer, M., Strebhardt, K., Hirai, H., Wilkinson, D.G., et al. (1996). Eph receptors and ligands comprise two major specificity subclasses and are reciprocally compartmentalized during embryogenesis. Neuron *17*, 9–19.

George, S.E., Simokat, K., Hardin, J., and Chisholm, A.D. (1998). The VAB-1 Eph receptor tyrosine kinase functions in neural and epithelial morphogenesis in *C. elegans*. Cell *92*, 633–643.

Guarente, L. (1993). Synthetic enhancement in gene interaction: a genetic tool come of age. Trends Genet. *9*, 395–399.

Henkemeyer, M., Orioli, D., Henderson, J.D., Saxton, T.M., Roder, J., Pawson, T., and Klein, R. (1996). Nuk controls pathfinding of commissural axons in the mammalian central nervous system. Cell *86*, 35–46.

Himanen, J.P., Henkemeyer, M., and Nikolov, D.B. (1998). Crystal structure of the ligand-binding domain of the receptor tyrosine kinase EphB2. Nature *396*, 486–491.

Hodgkin, J.A. (1997). Appendix 1: Genetics. In *C. elegans* II, D.L. Riddle, T. Blumenthal, B.J. Meyer, and J.R. Priess, eds. (Cold Spring Harbor, NY: Cold Spring Harbor Press), pp. 881–1048.

Holder, N., and Klein, R. (1999). Eph receptors and ephrins: effectors of morphogenesis. Development *126*, 2033–2044.

Holland, S.J., Gale, N.W., Mbalamu, G., Yancopoulos, G.D., Henkemeyer, M., and Pawson, T. (1996). Bidirectional signaling through the EPH-family receptor Nuk and its transmembrane ligands. Nature *383*, 722–725.

Kane, D.A., Hammerschmidt, M., Mullins, M.C., Maischein, H.M., Brand, M., van Eeden, F.J., Furutani-Seiki, M., Granato, M., Haffter, P., Heisenberg, C.P., et al. (1996). The zebrafish epiboly mutants. Development *123*, 47–55.

Krull, C.E., Lansford, R., Gale, N.W., Collazo, A., Marcelle, C., Yancopoulos, G.D., Fraser, S.E., and Bronner-Fraser, M. (1997). Interactions of Eph-related receptors and ligands confer rostrocaudal pattern to trunk neural crest migration. Curr. Biol. *7*, 571–580.

Maduro, M., and Pilgrim, D. (1995). Identification and cloning of *unc-119*, a gene expressed in the *Caenorhabditis elegans* nervous system. Genetics *141*, 977–988.

Mellitzer, G., Xu, Q., and Wilkinson, D.G. (1999). Eph receptors and ephrins restrict cell intermingling and communication. Nature *400*, 77–81.

Mello, C.C., Kramer, J.M., Stinchcomb, D., and Ambros, V. (1991). Efficient gene transfer in *C. elegans*: extrachromosomal maintenance and integration of transforming sequences. EMBO J. *10*, 3959–3970.

Mohler, W.A., Simske, J.S., Williams-Masson, E.M., Hardin, J.D., and White, J.G. (1998). Dynamics and ultrastructure of developmental cell fusions in the *Caenorhabditis elegans* hypodermis. Curr. Biol. *8*, 1087–1090.

Noselli, S., and Agnes, F. (1999). Roles of the JNK signaling pathway in Drosophila morphogenesis. Curr. Opin. Genet. Dev. *9*, 466–472.

Pandey, A., Lindberg, R.A., and Dixit, V. (1995). Receptor orphans find a family. Curr. Biol. *5*, 986–989.

Simons, K., and Ikonen, E. (1997). Functional rafts in cell membranes. Nature *387*, 569–572.

Smith, A., Robinson, V., Patel, K., and Wilkinson, D.G. (1997). The EphA4 and EphB1 receptor tyrosine kinases and ephrin-B2 ligand regulate targeted migration of branchial neural crest cells. Curr. Biol. *7*, 561–570.

Solnica-Krezel, L., Stemple, D.L., Mountcastle-Shah, E., Rangini, Z., Neuhauss, S.C., Malicki, J., Schier, A.F., Stainier, D.Y., Zwartkruis, F., Abdelilah, S., and Driever, W. (1996). Mutations affecting cell fates and cellular rearrangements during gastrulation in zebrafish. Development *123*, 67–80.

Stein, E., Lane, A.A., Cerretti, D.P., Schoecklmann, H.O., Schroff, A.D., Van Etten, R.L., and Daniel, T.O. (1998). Eph receptors discriminate specific ligand oligomers to determine alternative signaling complexes, attachment, and assembly responses. Genes Dev. *12*, 667–678.

Sulston, J.E., Schierenberg, E., White, J.G., and Thomson, J.N. (1983). The embryonic cell lineage of the nematode *Caenorhabditis elegans*. Dev. Biol. *100*, 64–119.

Thomas, S.M., and Brugge, J.S. (1997). Cellular functions regulated by Src family kinases. Annu. Rev. Cell Dev. Biol. *13*, 513–609.

Thomas, C., DeVries, P., Hardin, J., and White, J. (1996). Four-dimensional imaging: computer visualization of 3D movements in living specimens. Science *273*, 603–607.

Wang, H.U., Chen, Z.F., and Anderson, D.J. (1998). Molecular distinction and angiogenic interaction between embryonic arteries and veins revealed by ephrin-B2 and its receptor Eph-B4. Cell *93*, 741–753.

Wang, X., Roy, P.J., Holland, S.J., Zhang, L.W., Culotti, J., and Pawson, T. (1999). Multiple ephrins control cell organization in *C. elegans* through kinase-dependent and kinase-independent functions of the VAB-1 Eph receptor. Mol. Cell *4*, 903–913.

Williams-Masson, E.M., Malik, A.N., and Hardin, J. (1997). An actin-mediated two-step mechanism is required for ventral enclosure of the *C. elegans* hypodermis. Development *124*, 2889–2901.

Xu, Q., Mellitzer, G., Robinson, V., and Wilkinson, D.G. (1999). In vivo cell sorting in complementary segmental domains mediated by Eph receptors and ephrins. Nature *399*, 267–271.

GenBank Accession Number

The GenBank accession number for the *vab-2/efn-1* cDNA sequence is AF201079.